

RESEARCH

Open Access



Acquired sperm hypomethylation by gestational arsenic exposure is re-established in both the paternal and maternal genomes of post-epigenetic reprogramming embryos

Keiko Nohara^{1*}, Takehiro Suzuki¹, Kazuyuki Okamura¹, Tomoko Kawai² and Kazuhiko Nakabayashi²

Abstract

Background DNA methylation plays a crucial role in mammalian development. While methylome changes acquired in the parental genomes are believed to be erased by epigenetic reprogramming, accumulating evidence suggests that methylome changes in sperm caused by environmental factors are involved in the disease phenotypes of the offspring. These findings imply that acquired sperm methylome changes are transferred to the embryo after epigenetic reprogramming. However, our understanding of this process remains incomplete. Our previous study showed that arsenic exposure of F0 pregnant mice paternally increased tumor incidence in F2 offspring. The sperm methylome of arsenic-exposed F1 males exhibited characteristic features, including enrichment of hypomethylated cytosines at the promoters of retrotransposons LINEs and LTRs. Hypomethylation of retrotransposons is potentially detrimental. Determining whether these hypomethylation changes in sperm are transferred to the embryo is important in confirming the molecular pathway of intergenerational transmission of paternal effects of arsenic exposure.

Results We investigated the methylome of F2 male embryos after epigenetic reprogramming by reduced representation bisulfite sequencing (RRBS) and allele-specific analysis. To do so, embryos were obtained by crossing control or gestationally arsenic-exposed F1 males (C3H/HeN strain) with control females (C57BL/6 strain). The results revealed that the methylome of F2 embryos in the arsenic group was globally hypomethylated and enriched for hypomethylated cytosines in certain genomic regions, including LTR and LINE, as observed in F1 sperm of the arsenic group. Unexpectedly, the characteristic methylome features were detected not only in the paternal genome but also in the maternal genome of embryos. Furthermore, these methylation changes were found to rarely occur at the same positions between F1 sperm and F2 embryos.

*Correspondence:
Keiko Nohara
keikon@nies.go.jp

Full list of author information is available at the end of the article



© The Author(s) 2025. **Open Access** This article is licensed under a Creative Commons Attribution-NonCommercial-NoDerivatives 4.0 International License, which permits any non-commercial use, sharing, distribution and reproduction in any medium or format, as long as you give appropriate credit to the original author(s) and the source, provide a link to the Creative Commons licence, and indicate if you modified the licensed material. You do not have permission under this licence to share adapted material derived from this article or parts of it. The images or other third party material in this article are included in the article's Creative Commons licence, unless indicated otherwise in a credit line to the material. If material is not included in the article's Creative Commons licence and your intended use is not permitted by statutory regulation or exceeds the permitted use, you will need to obtain permission directly from the copyright holder. To view a copy of this licence, visit <http://creativecommons.org/licenses/by-nc-nd/4.0/>.

Conclusions The results of this study revealed that the characteristics of arsenic-induced methylome changes in F1 sperm are reproduced in both the paternal and maternal genomes of post-epigenetic reprogramming embryos. Furthermore, the results suggest that this re-establishment is achieved in collaboration with other factors that mediate region-specific methylation changes. These results also highlight the possibility that arsenic-induced sperm methylome changes could contribute to the development of disease predisposition in offspring.

Keywords Intergenerational transmission, Paternal effects, DNA methylation, Embryos, Sperm, Arsenic, Gestational exposure, Reduced representation bisulfite sequencing (RRBS), Allele-specific analysis

Background

Epigenetic reprogramming during embryogenesis is crucial for the development of mammalian zygotes into multicellular embryos [1, 2]. The earliest and most-studied epigenetic change during this process is the dynamic deletion and reconstitution of DNA methylation [1, 3]. Deletion of methylation has been recognized as a requirement not only for the acquisition of totipotency but also for the erasure of acquired epigenetic information. In mice, DNA methylation of the zygote genome is significantly reduced until the blastocyst implantation around embryonic day 3.5 (E3.5), and reconstitution is completed by approximately E7.5 [4, 5]. Later studies employing newly developed methods, such as genome-wide single-base resolution sequencing and allele-specific analysis, have further refined our understanding of DNA methylation reprogramming during embryogenesis [4–6].

On the other hand, numerous studies have reported that environmental factors affect offspring health through epigenetic modifications of the germ cells [7–11]. Sperm methylome changes by developmental and adult exposure to hazardous chemicals and improper nutrition have been implicated in the intergenerational transmission of disease phenotypes [12–17]. These findings may imply that environmentally acquired changes in the sperm methylome are transmitted to the embryos and contribute to the development of disease predisposition. However, our understanding of this process is still incomplete. Determining whether acquired methylome changes in sperm are transferred to the embryo is crucial to confirming the molecular process of intergenerational transmission of paternal health effects of arsenic.

Inorganic arsenic, a metalloid ubiquitously distributed in the environment, poses significant global health problems, including cancer, for millions of people in areas where highly contaminated groundwater is used for living and farming [18–21]. Waalkes et al. (2003) [22] reported that gestational arsenic exposure increased the incidence of hepatic tumors in males of C3H mice, which are prone to developing spontaneous hepatic tumors later in life.

Using the mouse model established by Waalkes' group, we previously found that exposure of F0 pregnant mice to arsenic increases the incidence of hepatic tumors in F2 males via the F1 male parents [23]. In F2 hepatic tumors

of the arsenic group, we identified two genes whose expression was upregulated and associated with DNA hypomethylation of the promoter regions, which were shown to be involved in hepatic tumor increase [24]. Furthermore, sperm of F1 mice gestationally exposed to arsenic exhibited genome-wide hypomethylation and a characteristic genomic region distribution of hypomethylated cytosines, particularly predominant in the promoter regions of retrotransposon LINEs and LTRs [25]. Hypomethylation of retrotransposon promoters is known to cause an increase in detrimental retrotransposition and can lead to various disorders, including cancer [26–28]. These findings highlight the next challenge of determining whether the acquired methylome changes are transmitted to embryo.

In this study, we investigated whether gestational arsenic exposure-induced DNA hypomethylation features in F1 sperm are transmitted to F2 male embryos. The results showed a unique manner in which acquired methylome characteristics in F1 sperm are re-established in the F2 embryos.

Methods

Experimental design

The design of the animal experiment is shown in Fig. 1. C3H/HeN F1 male offspring of the control group and the arsenic group were obtained as described previously [25]. Briefly, pregnant C3H/HeN mice (F0, purchased from CLEA Japan, Tokyo) in the control group were given free access to a standard diet (CA-1; CLEA Japan) and tap water. The mice in the arsenic group were given tap water containing 85 ppm sodium arsenite (Sigma) instead of tap water from gestational day (GD) 8 to 18. The experimental protocol caused no grossly recognized changes in F0, F1 or F2 mice. F1 males born to different dams, respectively, were crossed at 13–16 weeks old with C57BL/6 (B6) female mice (purchased from CLEA Japan, Tokyo) at 12–13 weeks old and embryos were obtained on embryonic day 7.5 (E7.5).

DNA and RNA were prepared from the homogenate of each embryo using an AllPrep DNA/RNA Mini Kits (Qiagen, the Netherlands). DNA was trapped and purified on the column according to the manufacturer's protocol. After sex determination of each embryo as described in the next section, DNA of 3–5 male embryos

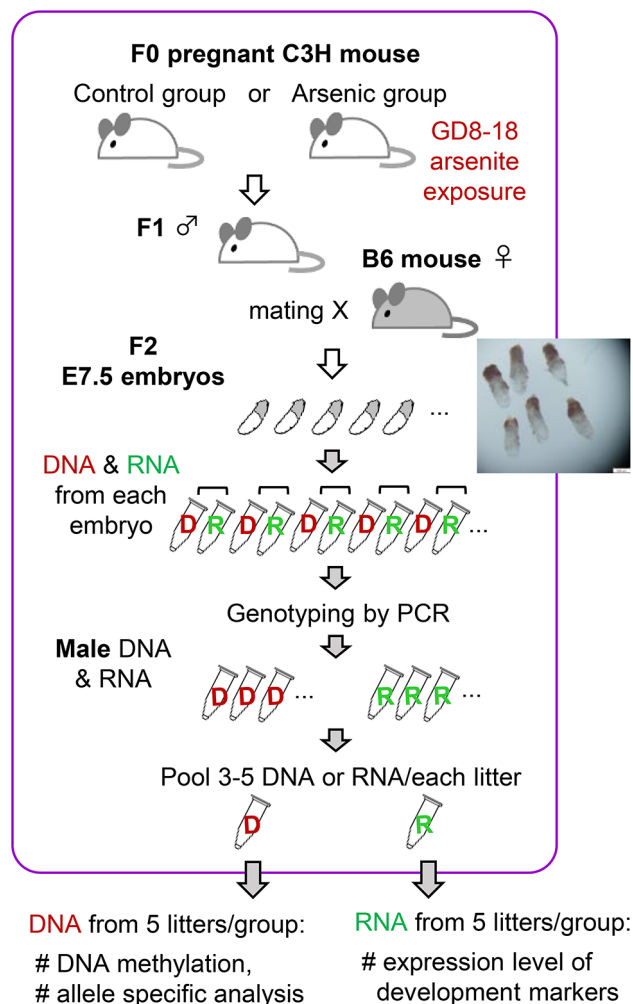


Fig. 1 Schematic diagram of experiments

from individual litters were pooled, and 5 pooled DNA samples from the control and arsenic group, respectively, were subjected to DNA methylation analysis. RNA was obtained in the flow-through fraction and concentrated using an RNeasy MinElute spin column (Qiagen) according to the manufacturer's instructions. RNA of 3–5 male embryos from individual litters were pooled and 5 pooled samples were analyzed for each group.

In a replication experiment (Exp. 2) on the F2 embryos, C3H/HeN F1 mice in the control and arsenic group were obtained as described above. Male F1 mice born to different dams were crossed at 13–14 weeks old with C57BL/6 female mice (11–12 weeks old) and embryos were obtained on E7.5. DNA and RNA from male embryos were prepared as describe above.

Mice were handled in a humane manner in accordance with the National Institute for Environmental Studies (NIES) guidelines for animal experiments. All the protocols for animal experiments were approved by the

Animal Care and Use Committee of the National Institute for Environmental Studies.

Sex determination

DNA sample obtained from each embryo was quantified using a Qubit dsDNA HS assay kit (Thermo Fisher Scientific, USA) and the quality was checked by gel electrophoresis. Sex determination was performed by PCR of embryo DNA with *Zfy* primers (5'-aagataagcttacataatcacatgga-3' and 5'-cctatgaaatcctttgctgcatgt-3'). The PCR mixture consisted of DNA (1.0 μ l), *Zfy* primer mixture (10 μ M each, 0.2 μ l), 10xLA PCR Buffer II (Mg^{2+} free, 1.0 μ l), 25 mM $MgCl_2$ (0.6 μ l), dNTP mixture (2.5 mM each, 0.2 μ l), H_2O (6.8 μ l), and rTaq 5U/ μ l (1.0 μ l). The buffer, $MgCl_2$, dNTP mixture and rTaq were obtained from Takara Bio Inc. (Japan). PCR was carried out on a GeneAmp PCR system 9700 (Applied Biosystems, USA) using the following condition: initial denaturation at 94 $^{\circ}C$ for 3 min, 35 cycles of 94 $^{\circ}C$ for 30 s, 64 $^{\circ}C$ for 30 s and 72 $^{\circ}C$ for 30 s, and final extension at 72 $^{\circ}C$ for 10 min. PCR products were examined by gel electrophoresis using 1.2% Agarose gel. The representative gel image was shown in Fig S1.

DNA methylation analysis by reduced representation bisulfite sequencing (RRBS) and determination of differentially methylated cytosines (DMCs) and differentially methylated regions (DMRs)

F2 embryo DNA were quantified using Genomic DNA ScreenTape and Genomic DNA reagent kit (Agilent Technologies) and used for preparation of RRBS libraries [29] with some modifications as described previously [25, 30]. The RRBS libraries were sequenced on an Illumina HiSeq X. Obtained reads were trimmed for adaptors using Trim Galore (http://www.bioinformatics.babraham.ac.uk/projects/trim_galore/) and mapped on the mouse reference genome (mm10) using the Bismark program [31]. The sequence data will be publicly available at Gene Expression Omnibus (GEO), NCBI with accession number GSE275185, and GSE275460 for Exp. 2, upon acceptance.

The mapped data were used for DNA methylation analysis by the methylKit package [32] on R. Detection of CpGs that are common in 10 samples in the control and arsenic groups and counting of reads with C (methylated) and with T (unmethylated) were carried out using the processBismarkAIn function in methylKit under the conditions of minimum coverage 10, minimum phred score 20 and destrand=false. Methylation difference and q value between the control and arsenic groups were determined for each CpG site using calculateDiffMeth function in methylKit. The list of CpGs was edited by excluding those assigned in chromosomes other than chr1-19, chrX and chrY, and was subjected to subsequent

analyses. The RRBS data of F1 sperm (GSE150650) obtained in our previous study [25] was edited in the same way and re-analyzed in the present study. Differentially methylated cytosines (DMCs) were defined as CpGs having $\geq 10\%$ methylation differences with $q < 0.01$ between the control and arsenic group unless otherwise stated. HypoDMCs and hyperDMCs are DMCs with lower and higher average methylation levels in the arsenic group compared to the control group, respectively.

Differentially methylated regions (DMRs) were selected using eDMR [33] utilizing the data obtained from methylKit by calculateDiffMeth analysis as described above. DMRs were defined as regions which contain three or more CpGs and at least one DMC (meth diff $\geq 10\%$) and having $\geq 10\%$ methylation difference with statistical significance. DMRs were also selected using tileMethylCounts function in methylKit as regions of 200 bps containing three or more CpGs and exhibiting $\geq 10\%$ methylation difference with statistical significance.

Principal component analysis (PCA) was performed on the mapped data using the prcomp function in R.

Annotation by HOMER, retrotransposon subfamily analysis and cCRE search

Each CpG was detailed annotated as per Table S2 using HOMER software (<http://homer.ucsd.edu/homer/>, v4.10) as described previously [25]. Analysis were performed with the default condition and the promoter region was set from -1 kb to $+100$ b from TSS. For the position analysis of DMCs in L1MdA subfamilies, a full-length L1MdA sequence was obtained as described previously [25] and more than 40 sequences containing hypo- or hyper-DMCs were randomly selected using SeqKit. The annotations of candidate ENCODE cis-regulatory elements (cCREs) combined from all cell types of mouse were downloaded from the UCSC Table Browser (https://genome.ucsc.edu/cgi-bin/hgTrackUi?hgsid=2339854132_0pTWnuoL7NrraXSVb6Vik7A8jUbT&db=mm10&c=chr16&g=encodeCcreCombined) [34] and the intersection with CpGs detected in the F2 embryos was captured using IntersectBed in bedtools (<https://bedtools.readthedocs.io/en/latest/>).

Allele-specific DNA methylation analysis

Sequence data for the C3H/HeN genome was obtained by whole genome sequencing of male liver DNA. The data will be publicly available at NCBI Sequence Read Archives (SRA) with accession number PRJNA1153074 upon acceptance. An N-masked reference genome that is based on the GRCm38/mm10 reference genome and N-masked at SNP positions between the GRCm38/mm10 and C3H/HeN genomes was produced from a variant call file made on Dragen (Illumina). RRBS data of F2 embryos were mapped to the N-masked reference genome and

paternal or maternal genome-specific splitting was performed by SNPsplit [35]. DNA methylation status was obtained using methRead and unite functions in a methylKit package. The condition `destrand = true` was applied, since more DMCs were detected under this condition compared to `destrand = false`. For comparison, RRBS data of F1 sperm [25] was also mapped to the N-masked reference genome and re-analyzed with the same conditions. For allele specific analysis, DMCs were set as CpGs having $\geq 2\%$ methylation differences with $q < 0.05$ between the control and arsenic group.

Real-time PCR analysis of developmental marker expression

RNA was reverse-transcribed using AMV Reverse Transcriptase XL (Takara Bio, Japan), and real-time PCR was performed with Light Cycler 480 SYBR Green I Master kit (Roche, Switzerland) on a Light Cycler 480 (Roche, Switzerland). Primers were designed using Primer3web (<http://primer3.ut.ee>). Primer sequences are shown in Table S1. The annealing temperature was 64°C for all the primers.

Statistical analysis

Differences in methylation levels between the control and arsenic groups were tested by Welch's t test and permutation test. Expression levels of developmental marker genes in the two groups were assessed by Student's t test. The probability of occurrence of hypo- and hyperDMCs compared to the occurrence of CpGs in each genomic region was assessed by Fisher's exact test.

Results

F2 embryos born to gestationally arsenic-exposed F1 males

The control or gestationally arsenic exposed F1 males (C3H strain) and C57BL/6 strain (B6) females were crossed and F2 male embryos were obtained on embryonic day 7.5 (E7.5), when DNA methylation reconstitution is completed via epigenetic reprogramming. The representative embryos (Fig. 1) were approximately 1.3–1.7 mm in length and morphologically appeared to be in the Mid Streak and Late Streak stages, according to the study by Downs and Davies [36]. Developmental stages were grossly similar in the embryos from the control and arsenic groups. There were no differences between the two groups in the expression levels of genes characteristic of the development of the endoderm (*Cer1*, *Sox17*), mesoderm (*Snail*, *Cdh11*) or extraembryonic ectoderm (*Elf5*) [37–39] on E7.5 (Fig. S1).

F2 embryos are DNA hypomethylated as are the F1 sperm of the arsenic group

DNA of F2 male embryos was subjected to RRBS analysis. MethylKit analysis of the sequence data (destrand = false) identified 2,137,827 CpGs common in all 10 samples in both the control and arsenic groups. A volcano plot illustrating the differences in methylation levels of each CpG between the two groups revealed a greater number of CpGs with significantly lowered DNA methylation in the arsenic group (Fig. 2A). HypoDMCs (blue dots) and hyperDMCs (red dots), which are hypo- and hypermethylated CpGs in the arsenic group compared to the control group ($\geq 10\%$ methylation difference, $q < 0.01$) were 18,366 and 9,963 in number, respectively (Fig. 2A). While the DNA methylation levels of whole genomes are generally stable and not widely altered by environmental factors, the average methylation level of all CpGs in the arsenic group (40.96%) was significantly lower than in the control group (41.56%) (Fig. 2B). Among the chromosomes, the CpGs methylation level was highest in chromosome Y (Fig. 2B). A predominance of hypoDMCs over hyperDMCs was observed across all chromosomes (Fig. 2C).

These features were reproducibly observed in another independent experiment (Exp. 2) on the methylome features of F2 embryos (Fig. S3A-C). The global hypomethylation and predominance of hypoDMCs over hyperDMCs are consistent with the results observed in the F1 sperm of the arsenic group found in our previous

study [25] and those reanalyzed in the present study (Fig. S4A, B).

HypoDMCs are enriched in LINE and LTR retrotransposons in F2 embryos as well as in F1 sperm of the arsenic group

All CpGs and DMCs were categorized into genomic regions as shown in Table S2, according to the detailed annotation by the HOMER software. The average methylation levels of all CpGs in individual regions were investigated, and the occurrence of CpGs and DMCs was compared in individual regions.

The sperm of gestationally arsenic-exposed F1 males showed highly significant hypomethylation and a profound overrepresentation of hypoDMCs in the LTR and LINE regions (Fig. S4C, D). Enrichment of hypoDMCs was also detected in the intergenic regions in the F1 sperm. As shown in Fig. 3A and B and Fig. S5A, significant hypomethylation and enrichment of hypoDMCs in the LTR and LINE regions were also detected in the F2 embryos. In addition, the exon, intron and intergenic regions were also enriched with hypoDMCs in the F2 embryos (Fig. 3B). The average methylation levels of hypo- and hyper-DMCs in individual regions are shown in Fig. 3C.

Analysis of differentially methylated regions (DMRs) using eDMR identified 4,071 hypoDMRs and 1,381 hyperDMRs. The distribution of these DMRs in individual regions (Fig. 3D) was similar to the distribution of DMCs (Fig. 3B), with a clearer predominance

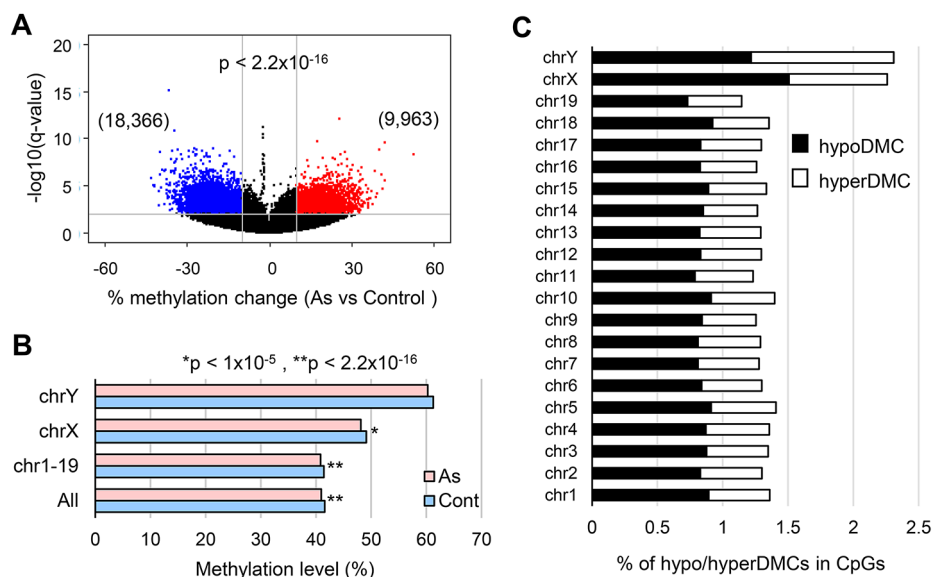


Fig. 2 Methylome profiles of F2 embryos in the control and arsenic groups. Identification of CpGs and calculation of methylation levels were performed using methylKit with the destrand=false condition. **A**) Volcano plot for the differences in the methylation levels of CpG sites between the control and arsenic groups. The x- and y-axes represent the difference in average methylation levels and q-values, respectively. P value for the difference in the methylation levels of all CpGs between the control and arsenic groups was assessed by permutation assay. **B**) Average methylation levels of all CpGs and those in autosomes and sex chromosomes in F2 embryos. The differences in the methylation levels between the control and arsenic groups were tested by Welch's t test. **C**) Percentages of hypo/hyperDMCs in all CpGs in each chromosome in F2 embryos. DMCs were defined as CpGs having $\geq 10\%$ methylation difference with $q < 0.01$

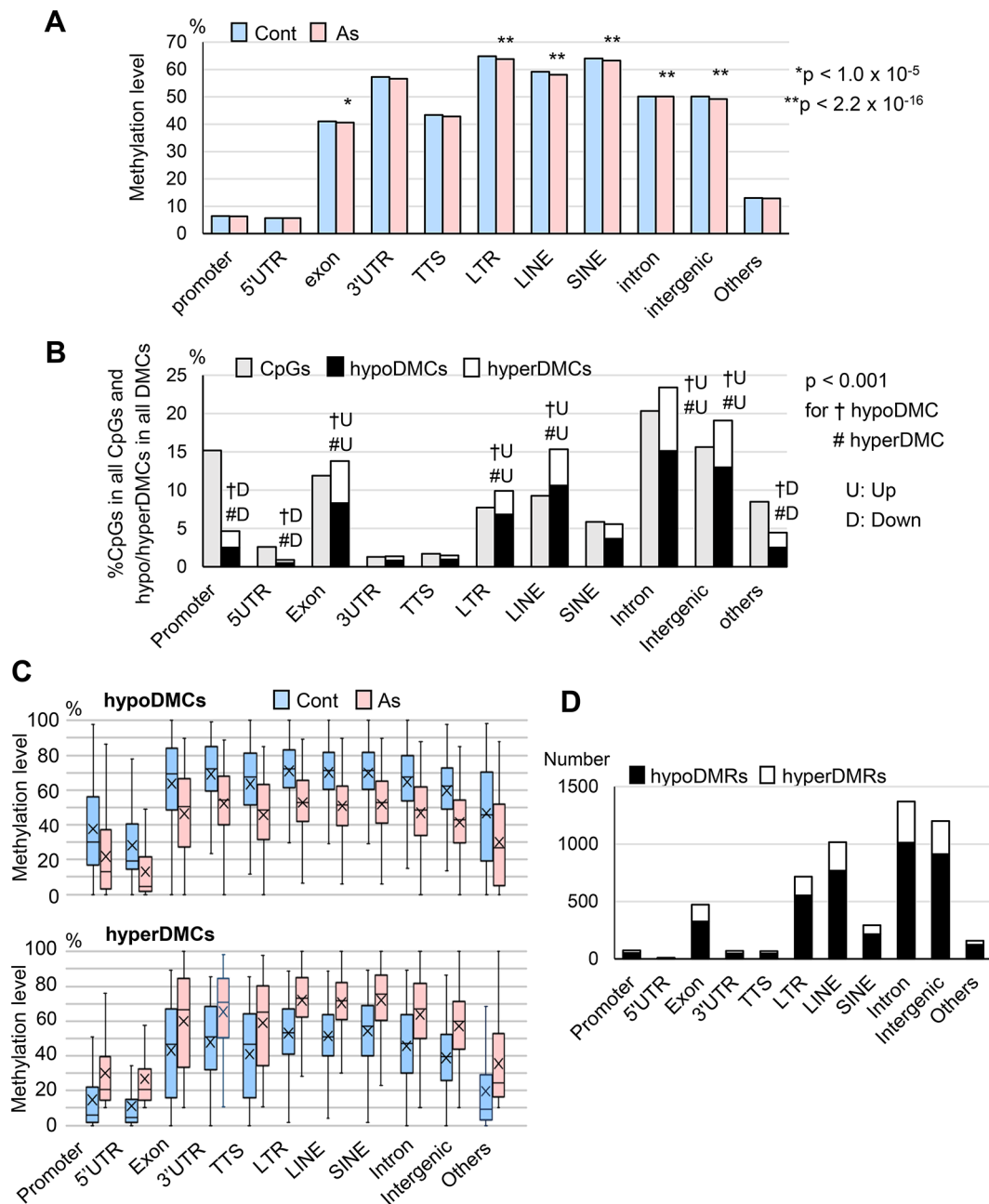


Fig. 3 Detailed annotation analysis of CpGs and DMCs of F2 embryos. **A**) Average methylation levels of all CpGs in the annotated regions. The differences in the methylation levels between the control and arsenic group were tested by Welch’s *t* test. **B**) Distribution (%) of detailed annotated regions among all CpGs (gray bars) and among all DMCs (hypoDMCs (black bars) plus hyperDMCs (white bars)). Methylation analysis was performed using methylKit with *dstrand*=false. DMC was defined as *q* < 0.01 and methylation difference ≥ 10%. For each region, difference in the occurrence of CpGs in all CpGs, and hypoDMCs in all hypoDMCs or hyperDMCs in all hyperDMCs, was assessed by Fisher’s exact test. Significantly increased (up) or decreased (down) DMCs (*p* < 0.001) were marked with † for hypoDMCs and # for hyperDMCs. U and D represent an up or down-regulated occurrence compared to CpGs, respectively. **C**) Box-and-whisker plots of methylation levels of hypo/hyperDMCs in the annotated regions. Crosses and bars in the box represent average and median values, respectively. **D**) Number of hypo/hyperDMRs assigned in the individual annotated regions

of hypoDMRs in the LTR, LINE, intron and intergenic regions. DMRs analyzed using the methylKit package also showed a similar region distribution (Fig. S5B). A highly similar distribution of DMCs and DMRs was observed in another independent experiment (Exp. 2) on F2 embryos (Fig. S3D - F).

HypoDMCs are enriched in the active LINE and LTR subfamilies in F2 embryos as in F1 sperm of the arsenic group

Among the LINES, L1MdA, L1MdGF and L1MdTF in the L1MdT subfamily contain transcriptionally active full-length elements [40, 41]. Hypermethylation at their promoters plays an essential role in repressing retrotransposition [26, 28]. Our previous study showed an overrepresentation of hypoDMCs in L1MdA and L1MdT in F1 sperm of the arsenic group [25]. In the present study, detailed annotation of DMCs in LINE subfamilies also showed significant hypomethylation of CpGs (Fig. 4A) and an overrepresentation of hypoDMCs (Fig. 4B) in the active LINE subfamilies in F2 embryos of the arsenic group. Positional analysis showed that hypo and hyperDMCs were enriched in the promoters of full-length L1MdA at and around -200 bp from 5'UTR (Fig. 4C), as was shown in F1 sperm [25].

Among the LTRs, all subfamilies, including the most transcriptionally active IAPs, were hypomethylated for CpGs (Fig. 4D) and enriched with hypoDMCs (Fig. 4E) as was shown in the F1 sperm of the arsenic group [25].

Number of DMCs is increased and distortion toward hypoDMC dominance is weakened in F2 embryos compared to F1 sperms of the arsenic group

The results described above clarified that the characteristic methylome features of F1 sperm, that is, the global hypomethylation and the predominance of hypoDMCs in the LTRs, LINES and intergenic regions, were also identified in the F2 embryos. Additionally, DMCs became enriched in the exon and intron regions in F2 embryos.

On the other hand, the percentage of DMCs in all CpGs increased in F2 embryos (Fig. 5A), and the distortion toward hypoDMC predominance was less prominent in F2 embryos than in F1 sperm (Fig. 5B). We also plotted the number of hypo- and hyperDMCs in individual regions with the number of candidate cis-regulatory elements (cCREs) that harbor the DMCs in F1 sperm and F2 embryos (Fig. 5C). The distal enhancer-like signature (dELS) was detected mainly in the intergenic and intron regions. The pie-charts in Fig. 5C show the percentage of individual elements in all DMCs. The most remarkable difference between F1 sperm and F2 embryos was the marked increase in the proportion of intron region hypoDMCs in F2 embryos, while the cCRE composition

in the intron region was not greatly altered between F1 sperm and F2 embryos.

Hypomethylation features of F1 sperm by arsenic exposure affect the methylome of both paternal and maternal genomes of F2 embryos

All the results obtained so far suggested that the sperm methylome feature endures epigenetic reprogramming and remains in the paternal genome of the embryos. This possibility was assessed by allele-specific analysis of RRBS data. Unexpectedly, the results showed that the average methylation levels of all CpGs are reduced not only in the paternal genome but also in the maternal genome (Table 1). The hypomethylation of both paternal and maternal genomes was confirmed in a replicate experiment, Exp. 2 (Table S3).

Figure 6 illustrates the distribution of CpGs and hypo-/hyperDMCs in the individual genomic regions. A predominance of hypoDMCs over hyperDMCs is observed in all regions of both the paternal and maternal genomes. The lack of statistically significant overrepresentation of DMCs in many genomic regions is attributed to the smaller number of CpGs identified in either genome. Despite this, a significant increase in hypoDMCs was detected in the LINE region in the maternal genome.

These results reveal that the acquired DNA methylome changes induced in F1 sperm by gestational arsenic exposure cause similar methylome changes in the paternal and maternal genomes of embryos after epigenetic reprogramming. This occurs despite the independent methylation modification processes in the paternal and maternal genomes. These findings suggest the involvement of other factors which affect the methylomes of both parent genomes in embryos.

Characteristic genomic region distribution of DMCs is reproducible in both F1 sperm and F2 embryos, but the positions of DMCs are not fixed

As described above, F1 sperm [25] and F2 embryos in the arsenic group exhibited highly reproducible methylome features in two independent experiments. These findings prompted us to investigate which methylation alterations are transmitted from F1 sperm to F2 embryos or which CpGs are predisposed to hypo- or hypermethylation in F1 sperm and F2 embryos by F0 gestational arsenic exposure. Contrary to expectations, the number of hypo- or hyperDMCs identified at the same positions was very limited between those of F1 sperm and F2 embryos (Table 2). Likewise, hypo- or hyperDMCs were rarely detected at the same position in the repeated experiments for both F1 sperm and F2 embryos (Table 2). These results suggest that methylome changes in sperm induced by gestational arsenic exposure are not directly inherited by the zygote genome but are re-established in

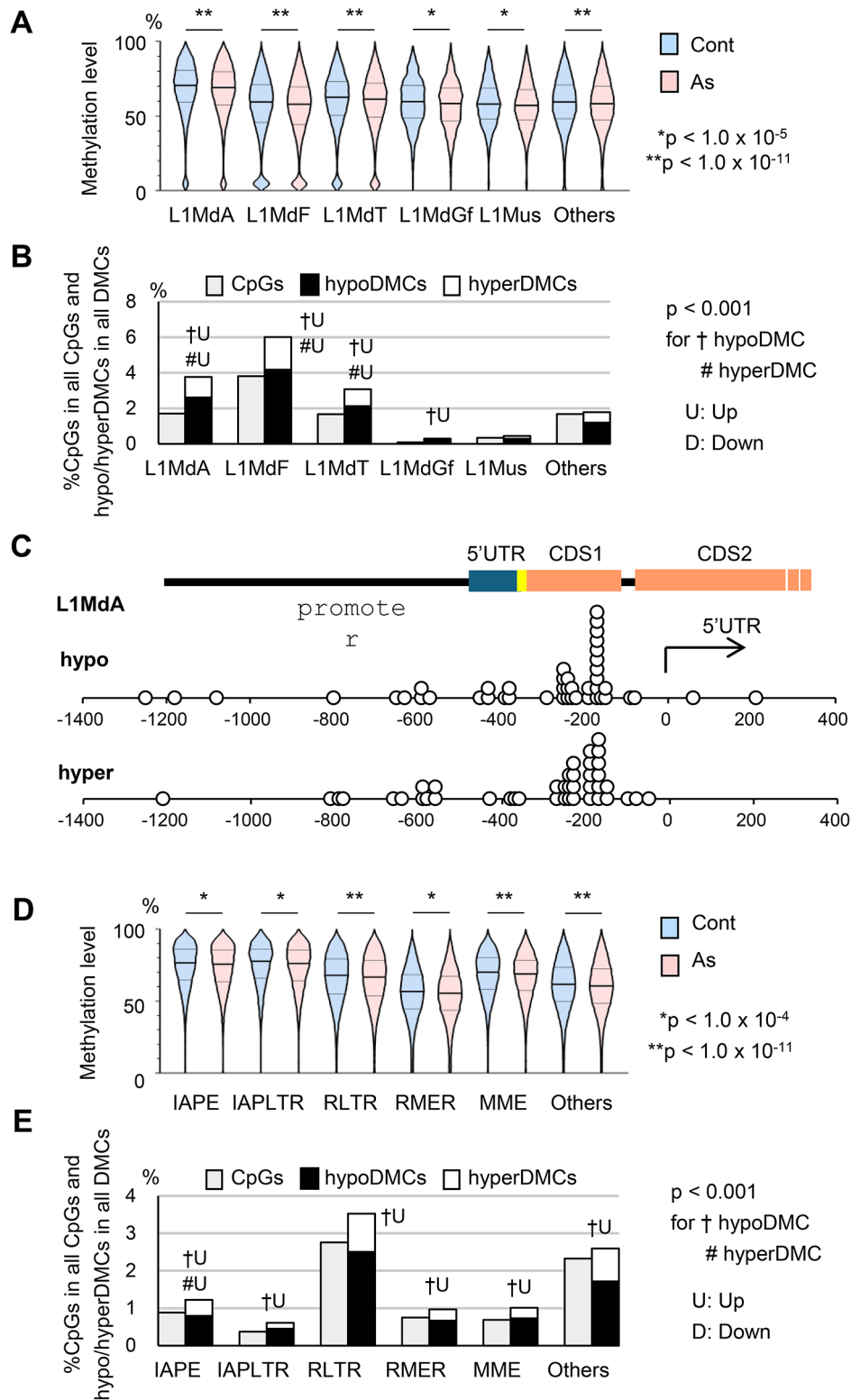


Fig. 4 Detailed annotation analysis of LINE and LTR subfamilies in F2 embryos. **A** and **D**) Violin plots of average methylation levels of all CpGs in each subfamily in LINE and LTR. Bold lines represent medians and thin lines represent quartiles. The differences in the methylation levels between the control and arsenic group were tested by Welch's *t* test. **B** and **E**) Distribution (%) of LINE and LTR subfamilies among all CpGs (gray bars) and among all DMCs (hypoDMCs (black bars) plus hyperDMCs (white bars)), respectively. Please see the legend in Fig. 3 for the method of statistics. **C**) The positions of hypo- and hyper-DMCs in the L1MdA subfamily

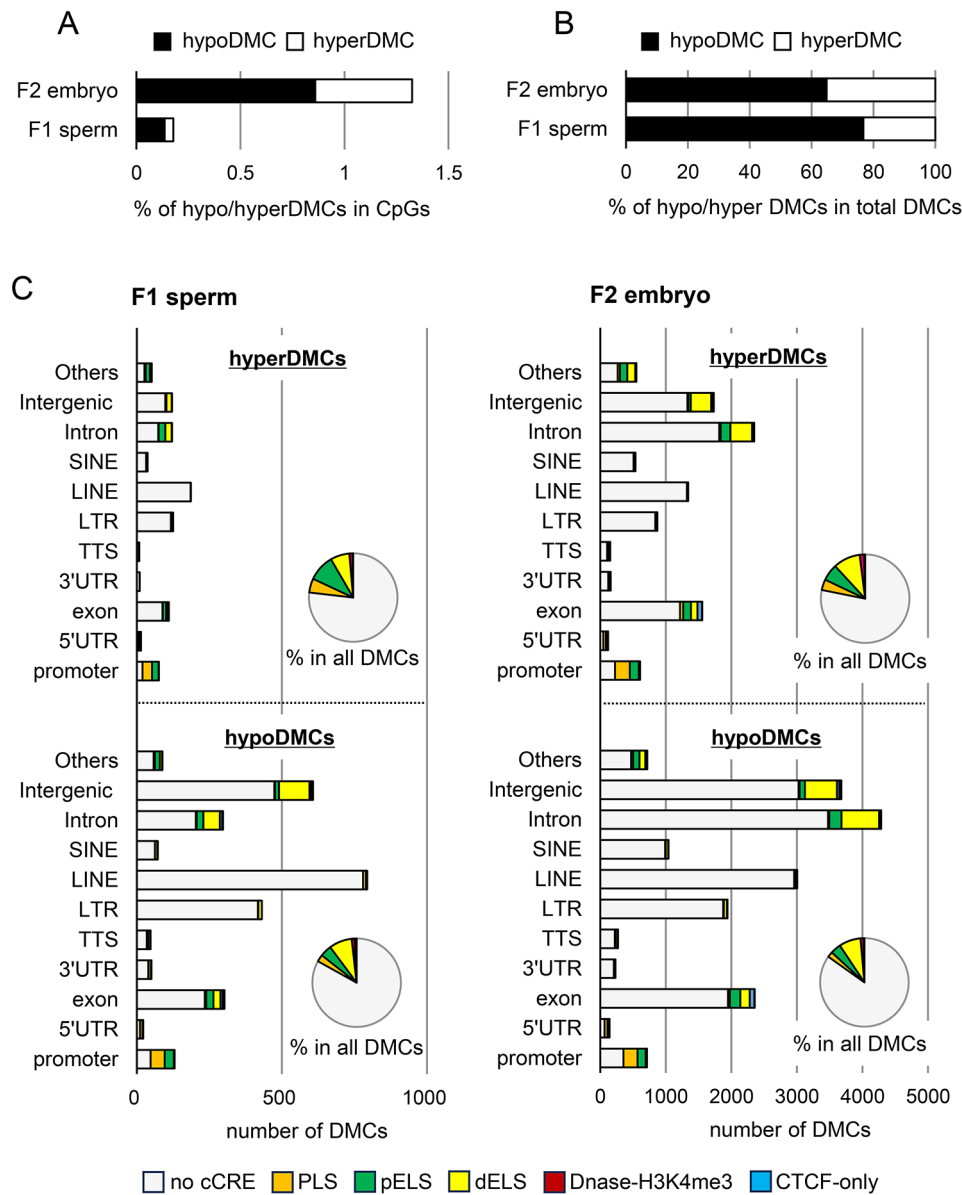


Fig. 5 DMCs in F1 sperm and F2 embryos. Comparison of % of hypo/hyperDMCs (methylation difference > 10%) in all CpGs (**A**) and the ratios of hypo- and hyper-DMCs (**B**) in F1 sperm and F2 embryos. **C** The number of DMCs including cCRE; PLS, promoter-like signature; pELS, proximal enhancer-like signature; dELS, distal enhancer-like signature

both parental genomes with region-specific frequencies, in collaboration with other factors.

DNA methylation of promoter and imprinted regions in F2 embryos

As shown in Fig. 3, the occurrence of DMCs in the promoter region is significantly lower than that of CpG, indicating that promoter region methylation is more refractory to the effect of arsenic exposure than other regions in F2 embryos. This feature is similar to that observed in F1 sperm.

Since environmental stimuli could affect imprinting gene expression [42, 43], we also investigated the

methylation levels of imprinted genes. The paternal imprinted regions, such as *Rasgrf1*, *H19 ICR* and *Gpr1/Zdbf2*, maintain high levels of CpG methylation in paternal genomes during epigenetic reprogramming [44]. The methylation levels of CpGs in these regions did not show any statistically significant changes in the embryos (Fig. S6).

Discussion

Using RRBS single-base resolution analysis, we investigated whether acquired DNA methylation changes in F1 sperm by gestational arsenic exposure are detected in F2 embryos after epigenetic reprogramming. The RRBS

Table 1 The methylation levels of CpGs in the paternal and maternal genomes of F2 embryos *

Genomes	Number of CpGs	Methylation level of CpGs (%)		
		Control	Arsenic	p value**
F2 Embryo Genome-unspecified	1,410,646	44.36	43.66	$<2.2 \times 10^{-16}$
Paternal	64,611	51.57	50.73	1.6×10^{-8}
Maternal	93,966	52.19	51.43	2.7×10^{-9}
F1 sperm	1,303,934	45.90	45.65	3.7×10^{-6}

* An N-masked reference genome was produced based on the GRCm38/mm10 and N-masking at SNP positions between GRCm38/mm10 and C3H/HeN genomes. RRBS data of F2 embryos were mapped to the N-masked reference genome and paternal or maternal genome-specific splitting was performed by SNPsplit. For comparison, RRBS data of F1 sperm was also mapped to the N-masked reference genome. Please see the Methods section for the analysis conditions

** The difference between the methylation levels in the two groups was assessed by Welch's t test

method measures methylation levels of 5–10% of all CpGs in the genome by effectively capturing CpGs and has been adopted in many studies [30, 45]. Smith et al. [4]

clarified precise methylome changes including those in retrotransposon regions in early embryogenesis of mice by RRBS analysis.

As shown in Fig. S7, principal component analysis (PCA) did not detect clear differences in the methylomes of F1 sperm or F2 embryos between the control and arsenic groups. On the other hand, analyses focusing on the methylation levels and region-specific distribution of hypoDMCs revealed statistically significant differences between the control and arsenic groups in both F1 sperm in our previous study [25] and F2 embryos in this study.

The present study revealed that the characteristic hypomethylation in F1 sperm by gestational arsenic exposure is observed in both the paternal and maternal genomes of F2 embryos after epigenetic reprogramming. While DNA methylation is one of the candidates for mediators in the intergenerational transmission of paternal effects, this study suggests that methylome alterations in arsenic-exposed sperm are not directly inherited by embryos. Instead, these alterations are thought to be

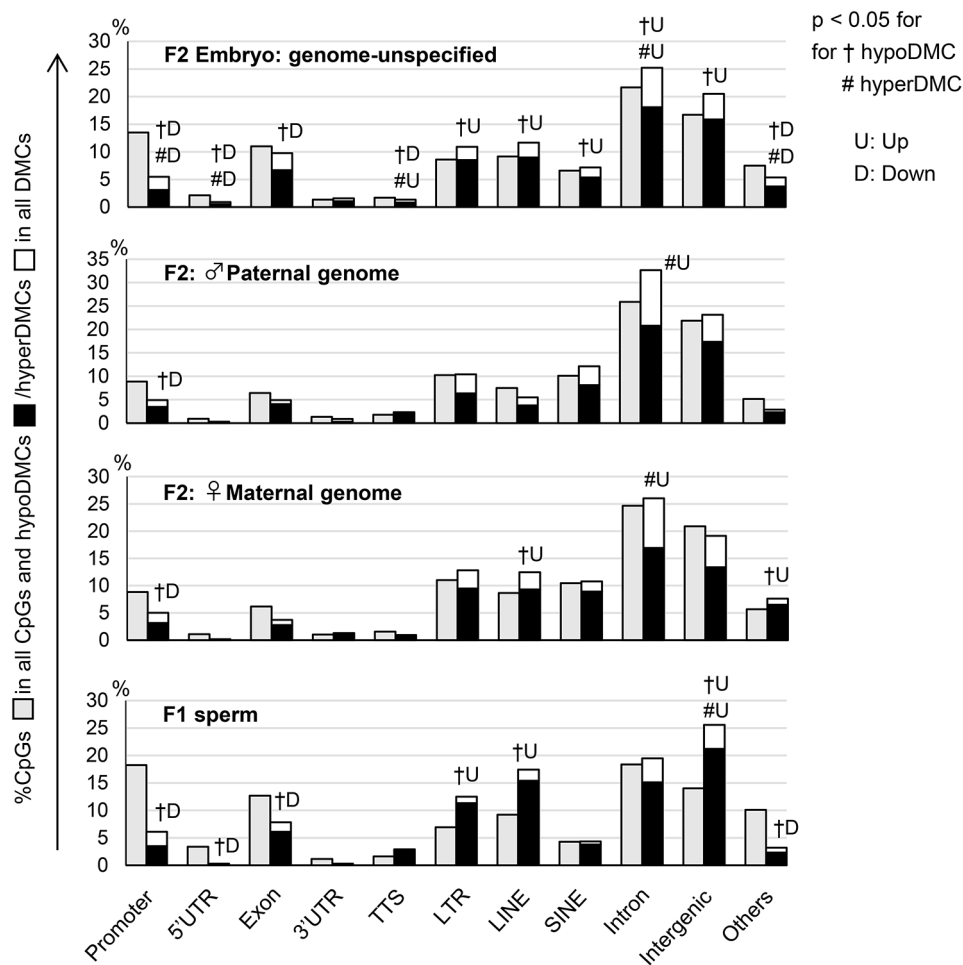


Fig. 6 Genome-specific analysis of methylome changes in the paternal and maternal genomes of F2 embryos. For comparison, RRBS data of F1 sperm was also analyzed in the same condition for comparison. Methylation analysis was performed using methylKit with destrand = true. DMC was defined as $q < 0.05$ and methylation difference $\geq 2\%$. Please see the legend in Fig. 3 for descriptions of the figures

Table 2 The number of DMCs commonly detected in the same positions in two independent experiments*

	F1 Sperm		F1 Sperm (Exp. 1) & F2 Embryo (Exp. 1)		F2 Embryo	
HypoDMC	Exp. 1	2,837	F1 Sperm	2,742	Exp. 1	18,423
	Exp. 2	1,503	F2 Embryo	17,648	Exp. 2	5,336
	Common	21	Common	48	Common	165
HyperDMC	Exp. 1	690	F1 Sperm	572	Exp. 1	8,896
	Exp. 2	402	F2 Embryo	8,670	Exp. 2	2,750
	Common	0	Common	6	Common	85

* CpGs that are common in 20 samples in the two experiments were selected using methylKit and DMCs (methylation difference $\geq 10\%$ with q value < 0.01) were detected in the common CpGs for each experiment. The number of DMCs in the same positions and different positions between the two experiments are indicated. F1 sperm DMCs were obtained using the RRBS data of F1 sperm (GEO150650) and of another independent experiment (GSE150500) (Nohara et al. 2020)

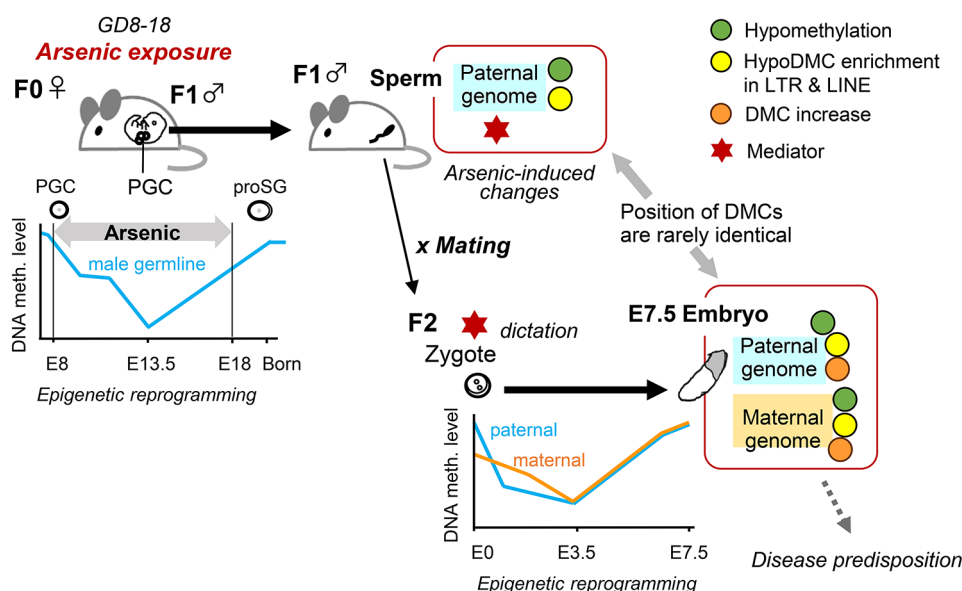


Fig. 7 Schematic summary on the transmission of altered methylome characteristics of F1 sperm into F2 embryos. The acquired methylome characteristics in F1 sperm by gestational arsenic exposure are passed on to both parental genomes of F2 embryos by unidentified mechanisms

stochastically induced with higher frequencies in certain regions, such as LINE and LTR, during epigenetic reprogramming in collaboration with other factors. The factors (mediator) may be affected in sperm by gestational arsenic exposure, transferred to embryos, and dictate region-specific methylation changes in both parental genomes, possibly depending on sequence characteristics. However, the possibility of direct transmission of methylome alterations from zygote to embryo cannot be excluded, since we currently lack the methods to examine the methylomes of sperm and embryo in a real parent-offspring relationship. Further mechanistic evidence will be required to determine the transmission pathway.

Figure 7 summarizes the results of this study and hypothesis on the unidentified mechanism.

Interestingly, a recent study by Chan et al. [46] reported in mice that feeding folic acid deficient or supplemented diet to dams and F1 male offspring caused transgenerational hypomethylation of active LINE subfamilies in sperm of F1, F2 and F3 generations. Folate is a cofactor in

the methionine metabolism. Furthermore, the study [46] reported that DMCs rarely occurred in the same positions in sperm between F1 and F2 or F2 and F3. These methylation changes in sperm may not be inherited in the same positions in embryos, as observed in the present study.

Retrotransposition of LTRs and LINEs is known to lead to various disorders, including cancer [26–28]. LINE-1 transposition is involved in activation of hepatocellular carcinoma [47]. Furthermore, LTRs and LINEs are crucially involved in pre- and post-implantation development [48, 49]. Thus, further investigation on the involvement of retrotransposon hypomethylation will be required to determine the trajectory of intergenerational transmission of paternal tumor-augmenting effect of arsenic.

After fertilization, the genomes from sperm and oocytes are demethylated through TET3-mediated active demethylation and replication-mediated passive demethylation with different kinetics in the embryos [5, 50–52].

Then paternal and maternal genomes are re-methylated by Dnmt3a/3b and Dnmt1 and acquire similar methylome patterns to each other [6, 53–56]. The function of these methylation-related enzymes would be among the final targets of hypomethylation induction in the embryos by arsenic exposure.

As mediators of paternal transgenerational inheritance, sperm non-coding RNAs, including tRNA fragments (tsRNAs), miRNAs, rRNA fragments (rsRNAs) and long non-coding RNAs have been implicated in transmission of information acquired from the environment to zygotes (57–58). While sperm histones are largely replaced by protamines, small amounts of histones are retained in mature sperm, mainly at specific promoter regions [59, 60] and their modifications are implicated in the intergenerational transmission [15, 61]. Chromosomal interactions by insulator CTCF and transcription factors in sperm are suggested to be maintained in the embryos and involved in the intergenerational transmission [62]. Since histone modifications [52], transcription factors having sequence-dependent CpG-binding activity [63] and non-coding RNAs, such as miRNA [64], are known to be crucial to organization and function of DNMTs, interaction with these factors may be involved in transmission of methylome information from sperm to embryos as ‘mediator’.

Inorganic arsenic is reported to affect methionine metabolism by consuming the methyl donor S-adenosyl-methionine by methylation of itself [18]. Disturbance of methionine metabolism may be commonly involved in the hypomethylation induction by arsenic exposure and folic acid deficient or supplemented diet feeding reported by Chang et al. [46]. Arsenic is also known to directly interact with the thiol group, is replaced with zinc ion in zinc finger proteins and indirectly induces oxidative stress and a variety of signaling pathways in a tissue/cell type-specific manner [18, 19, 65]. Gestationally exposed arsenic reaches the fetus tissues [66] and could affect these factors and pathways in the F1 offspring and the germ cells. Since a variety of environmental factors also interact with these factors/pathways, such as oxidative stress, the findings obtained in the present study may provide clues to understanding the intergenerational transmission of paternal effects by broader environmental factors.

Conclusions

The results of this study revealed that the characteristics of arsenic-induced methylome changes in F1 sperm are re-established in both the paternal and maternal genomes of post-epigenetic reprogramming F2 embryos. Furthermore, methylome changes, including hypomethylation of LTRs and LINEs, are suggested to be established in the embryo in concert with other factors that

dictate methylation changes at genomic region-specific frequencies. The results indicate the possibility that the arsenic-induced methylome changes in sperm can be involved in the development of disease predisposition in the offspring. The findings also provide new insight into the intergenerational transmission of paternal environmental effects.

Supplementary Information

The online version contains supplementary material available at <https://doi.org/10.1186/s13072-025-00569-7>.

Supplementary Material 1

Acknowledgements

The authors wish to thank Ms. H. Murai, Ms. M. Sato (NIES) and Dr Keisuke Ishiwata (NCCHD) for their excellent technical assistance, the staff of the Animal Care company for their assistance in animal experiments, and Dr Nobuyoshi Nakajima and Dr Shigekatsu Suzuki (NIES) for their kind advice on sequence analysis. We wish to thank Dr Kenji Ichiyanagi (Nagoya University) for his meaningful discussions on epigenetic inheritance and Dr Kenichiro Hata (NCCHD, Gunma University) for his encouragement.

Author contributions

K.Nohara designed this project, performed experiments and analysis, and wrote the manuscript. T.S. performed experiments and analysis. K.O. performed experiments. T.K. performed analysis. K.Nakabayashi designed the sequence analysis, and performed experiments and analysis. All authors read and approved the final manuscript.

Funding

This study was partly supported by the National Institute for Environmental Studies (1620AA041) and Grant-in-Aid for Scientific Research (15K15246, 18K19860, Nohara) from the Ministry of Education, Culture, Sports, Science and Technology of Japan.

Data availability

The RRBS data on the F2 embryos will be publicly available at GEO with accession number GSE275185, and GSE275460 for Exp. 2, upon acceptance. The RRBS data on the F1 sperm are available at GEO with accession number GSE150500 and 150650 (Nohara et al. 2020). The WGS data for C3H/HeN genome will be available at Sequence Read Archives (SRA), NCBI with accession number PRJNA1153074 upon acceptance.

Declarations

Ethics approval and consent to participate

All the protocols for animal experiments were approved by the Animal Care and Use Committee of the National Institute for Environmental Studies.

Consent for publication

Not applicable.

Competing interests

The authors declare no competing interests.

Author details

¹Health and Environmental Risk Division, National Institute for Environmental Studies, Tsukuba 305- 8506, Japan

²Department of Maternal-Fetal Biology, National Center for Child Health and Development, Tokyo 157-8535, Japan

Received: 18 September 2024 / Accepted: 6 January 2025

Published online: 16 January 2025

References

1. Reik W, Dean W, Walter J. Epigenetic reprogramming in mammalian development. *Science*. 2001;293:1089–93.
2. Li E. Chromatin modification and epigenetic reprogramming in mammalian development. *Nat Rev Genet*. 2002;3(9):662–73.
3. Smith ZD, Meissner A. DNA methylation: roles in mammalian development. *Nat Rev Genet*. 2013;14(3):204–20.
4. Smith ZD, Chan MM, Mikkelsen TS, Gu H, Gnirke A, Regev A, et al. A unique regulatory phase of DNA methylation in the early mammalian embryo. *Nature*. 2012;484(7394):339–44.
5. Wang L, Zhang J, Duan J, Gao X, Zhu W, Lu X, et al. Programming and inheritance of parental DNA methylomes in mammals. *Cell*. 2014;157(4):979–91.
6. Zhang Y, Xiang Y, Yin Q, Du Z, Peng X, Wang Q, et al. Dynamic epigenomic landscapes during early lineage specification in mouse embryos. *Nat Genet*. 2017;50(1):96–105.
7. Anway M, Cupp A, Uzumcu M, Skinner M. Epigenetic transgenerational actions of endocrine disruptors and male fertility. *Science*. 2005;308.
8. Barouki R, Melen E, Herceg Z, Beckers J, Chen J, Karagas M, et al. Epigenetics as a mechanism linking developmental exposures to long-term toxicity. *Environ Int*. 2018;114:77–86.
9. Boskovic A, Rando OJ. Transgenerational epigenetic inheritance. *Annu Rev Genet*. 2018;52:21–41.
10. Cavalli G, Heard E. Advances in epigenetics link genetics to the environment and disease. *Nature*. 2019;571(7766):489–99.
11. Breton CV, Landon R, Kahn LG, Enlow MB, Peterson AK, Bastain T, et al. Exploring the evidence for epigenetic regulation of environmental influences on child health across generations. *Commun Biol*. 2021;4(1):769.
12. Radford EJ, Ito M, Shi H, Corish JA, Yamazawa K, Isganaitis E, et al. In utero effects. In utero undernourishment perturbs the adult sperm methylome and intergenerational metabolism. *Science*. 2014;345(6198):1255903.
13. Champroux A, Cocquet J, Henry-Berger J, Drevet JR, Kocer A. A decade of exploring the mammalian sperm Epigenome: paternal epigenetic and transgenerational inheritance. *Front Cell Dev Biol*. 2018;6:50.
14. Illum LRH, Bak ST, Lund S, Nielsen AL. DNA methylation in epigenetic inheritance of metabolic diseases through the male germ line. *J Mol Endocrinol*. 2018;60(2):R39–56.
15. Lisner A, Kimmins S. Emerging evidence that the mammalian sperm epigenome serves as a template for embryo development. *Nat Commun*. 2023;14(1):2142.
16. Wang S, Wu J, Chen Z, Wu W, Lu L, Cheng Y, et al. DNA methylation reprogramming mediates transgenerational diabetogenic effect induced by early-life p,p'-DDE exposure. *Chemosphere*. 2024;349:140907.
17. Haberman M, Menashe T, Cohen N, Kisliouk T, Yacid T, Marco A, et al. Paternal high-fat diet affects weight and DNA methylation of their offspring. *Sci Rep*. 2024;14(1):19874.
18. Hughes MF, Beck BD, Chen Y, Lewis AS, Thomas DJ. Arsenic exposure and toxicology: a historical perspective. *Toxicol Sci*. 2011;123(2):305–32.
19. Martinez VD, Lam WL. Health effects Associated with pre- and perinatal exposure to Arsenic. *Front Genet*. 2021;12:664717.
20. Rahman A, Islam MS, Tony SR, Siddique AE, Mondal V, Hosen Z, et al. T helper 2-driven immune dysfunction in chronic arsenic-exposed individuals and its link to the features of allergic asthma. *Toxicol Appl Pharmacol*. 2021;420:115532.
21. Young JL, States LC. JC. Impact of prenatal arsenic exposure on chronic adult diseases. *Syst Biology Reproductive Med*. 2018;64.
22. Waalkes MP, Ward JM, Liu J, Diwan BA. Transplacental carcinogenicity of inorganic arsenic in the drinking water: induction of hepatic, ovarian, pulmonary, and adrenal tumors in mice. *Toxicol Appl Pharmacol*. 2003;186(1):7–17.
23. Nohara K, Okamura K, Suzuki T, Murai H, Ito T, Shinjo K, et al. Augmenting effects of gestational arsenite exposure of C3H mice on the hepatic tumors of the F(2) male offspring via the F(1) male offspring. *J Appl Toxicol*. 2016;36(1):105–12.
24. Okamura K, Nakabayashi K, Kawai T, Suzuki T, Sano T, Hata K, et al. DNA methylation changes involved in the tumor increase in F2 males born to gestationally arsenite-exposed F1 male mice. *Cancer Sci*. 2019;110(8):2629–42.
25. Nohara K, Nakabayashi K, Okamura K, Suzuki T, Suzuki S, Hata K. Gestational arsenic exposure induces site-specific DNA hypomethylation in active retrotransposon subfamilies in offspring sperm in mice. *Epigenetics Chromatin*. 2020;13(1):53.
26. Goodier JL, Kazazian HH. Jr. Retrotransposons revisited: the restraint and rehabilitation of parasites. *Cell*. 2008;135(1):23–35.
27. Thompson PJ, Macfarlan TS, Lorincz MC. Long terminal repeats: from parasitic elements to Building blocks of the Transcriptional Regulatory Repertoire. *Mol Cell*. 2016;62(5):766–76.
28. Pappalardo XG, Barra V. Losing DNA methylation at repetitive elements and breaking bad. *Epigenetics Chromatin*. 2021;14(1):25.
29. Boyle P, Clement K, Gu H, Smith ZD, Ziller M, Fostel JL, et al. Gel-free multiplexed reduced representation bisulfite sequencing for large-scale DNA methylation profiling. *Genome Biol*. 2012;13(10):R92.
30. Nakabayashi K, Yamamura M, Hasegawa K, Hata K. Reduced representation bisulfite sequencing (RRBS). *Methods Mol Biol*. 2023;2577:39–51.
31. Krueger F, Andrews SR. Bismark: a flexible aligner and methylation caller for Bisulfite-Seq applications. *Bioinformatics*. 2011;27(11):1571–2.
32. Akalin A, Kormaksson M, Li S, Garrett-Bakelman FE, Figueroa ME, Melnick A, et al. methylKit: a comprehensive R package for the analysis of genome-wide DNA methylation profiles. *Genome Biol*. 2012;13(10):R87.
33. Li S, Garrett-Bakelman FE, Akalin A, Zumbo P, Levine R, To BL, Ian D, Lewis ID, et al. An optimized algorithm for detecting and annotating regional differential methylation. *BMC Bioinformatics*. 2013;14:510.
34. Consortium EP, Moore JE, Purcaro MJ, Pratt HE, Epstein CB, Shores N, et al. Expanded encyclopaedias of DNA elements in the human and mouse genomes. *Nature*. 2020;583(7818):699–710.
35. Krueger F, Andrews SR, SNPsplit. Allele-specific splitting of alignments between genomes with known SNP genotypes. *F1000Res*. 2016;5:1479.
36. Downs TM, Davies T. Staging of gastrulating mouse embryos by morphological landmarks in the dissecting microscope. *Development*. 1993;118:1255–66.
37. Argelaguet R, Clark SJ, Mohammed H, Stapel LC, Krueger C, Kapourian CA, et al. Multi-omics profiling of mouse gastrulation at single-cell resolution. *Nature*. 2019;576(7787):487–91.
38. Pijuan-Sala B, Griffiths JA, Guibentif C, Hiscock TW, Jawaid W, Calero-Nieto FJ, et al. A single-cell molecular map of mouse gastrulation and early organogenesis. *Nature*. 2019;566(7745):490–5.
39. Mittnenzweig M, Maysbar Y, Cheng S, Ben-Yair R, Hadas R, Rais Y, et al. A single-embryo, single-cell time-resolved model for mouse gastrulation. *Cell*. 2021;184(11):2825–e4222.
40. Goodier JL, Ostertag EM, Du K, Kazazian JHH. A novel active L1 retrotransposon subfamily in the mouse. *Genome Res*. 2001;11:1677–85.
41. Sookdeo A, Hepp CM, McClure MA, Boissinot S. Revisiting the evolution of mouse LINE-1 in the genomic era. *Mob DNA*. 2013;4:15.
42. Rando OJ. Intergenerational Transfer of Epigenetic Information in sperm. *Cold Spring Harb Perspect Med*. 2016;6(5).
43. Kanatsu-Shinohara M, Shiromoto Y, Ogonuki N, Inoue K, Hattori S, Miura K et al. Intracytoplasmic sperm injection induces transgenerational abnormalities in mice. *J Clin Invest*. 2023;133(22).
44. Xie W, Barr CL, Kim A, Yue F, Lee AY, Eubanks J, et al. Base-resolution analyses of sequence and parent-of-origin dependent DNA methylation in the mouse genome. *Cell*. 2012;148(4):816–31.
45. Wan M, Bell DA. Analysis of genome-wide methylation using reduced representation bisulfite sequencing (RRBS) technology. *Epigenetics Methods*. 2020;141–56.
46. Chan D, Ly L, Rebollo EMD, Martel J, Landry M, Scott-Boyer MP, et al. Transgenerational impact of grand-paternal lifetime exposures to both folic acid deficiency and supplementation on genome-wide DNA methylation in male germ cells. *Andrology*. 2023;11(5):927–42.
47. Shukla R, Upton KR, Munoz-Lopez M, Gerhardt DJ, Fisher ME, Nguyen T, et al. Endogenous retrotransposition activates oncogenic pathways in hepatocellular carcinoma. *Cell*. 2013;153(1):101–11.
48. Kohrausch FB, Berteli TS, Wang F, Navarro PA, Keefe DL. Control of LINE-1 Expression Maintains Genome Integrity in Germline and early embryo development. *Reprod Sci*. 2022;29(2):328–40.
49. Wang J, Lu X, Zhang W, Liu GH. Endogenous retroviruses in development and health. *Trends Microbiol*. 2024;32(4):342–54.
50. Guo F, Li X, Liang D, Li T, Zhu P, Guo H, et al. Active and passive demethylation of male and female pronuclear DNA in the mammalian zygote. *Cell Stem Cell*. 2014;15(4):447–59.
51. Shen L, Inoue A, He J, Liu Y, Lu F, Zhang Y. Tet3 and DNA replication mediate demethylation of both the maternal and paternal genomes in mouse zygotes. *Cell Stem Cell*. 2014;15(4):459–71.
52. Chen Z, Zhang Y. Role of mammalian DNA methyltransferases in Development. *Annu Rev Biochem*. 2020;89:135–58.

53. Okano M, Bell DW, Haber DA, Li E. DNA methyltransferases Dnmt3a and Dnmt3b are essential for De Novo methylation and mammalian development. *Cell*. 1999;99:247–57.
54. Kaneda M, Okano M, Hata K, Sado T, Tsujimoto N, Li E, et al. Essential role for de novo DNA methyltransferase Dnmt3a in paternal and maternal imprinting. *Nature*. 2004;429:900–3.
55. Messerschmidt DM, Knowles BB, Solter D. DNA methylation dynamics during epigenetic reprogramming in the germline and preimplantation embryos. *Genes Dev*. 2014;28(8):812–28.
56. Dahlet T, Argueso Lleida A, Al Adhami H, Dumas M, Bender A, Ngondo RP, et al. Genome-wide analysis in the mouse embryo reveals the importance of DNA methylation for transcription integrity. *Nat Commun*. 2020;11(1):3153.
57. Zhang Y, Shi J, Rassoulzadegan M, Tuorto F, Chen Q. Sperm RNA code programmes the metabolic health of offspring. *Nat Rev Endocrinol*. 2019;15(8):489–98.
58. Tomar A, Gomez-Velazquez M, Gerlini R, Comas-Armangue G, Makharadze L, Kolbe T, et al. Epigenetic inheritance of diet-induced and sperm-borne mitochondrial RNAs. *Nature*. 2024;630(8017):720–7.
59. Yoshida K, Muratani M, Araki H, Miura F, Suzuki T, Dohmae N, et al. Mapping of histone-binding sites in histone replacement-completed spermatozoa. *Nat Commun*. 2018;9(1):3885.
60. Yamaguchi K, Hada M, Fukuda Y, Inoue E, Makino Y, Katou Y, et al. Re-evaluating the localization of sperm-retained histones revealed the modification-dependent Accumulation in Specific Genome regions. *Cell Rep*. 2018;23(13):3920–32.
61. Sakashita A, Ooga M, Otsuka K, Maezawa S, Takeuchi C, Wakayama S, et al. Polycomb protein SCML2 mediates paternal epigenetic inheritance through sperm chromatin. *Nucleic Acids Res*. 2023;51(13):6668–83.
62. Jung YH, Kremsky I, Gold HB, Rowley MJ, Punyawai K, Buonanotte A, et al. Maintenance of CTCF- and transcription factor-mediated interactions from the gametes to the early mouse embryo. *Mol Cell*. 2019;75(1):154–71. e5.
63. Zhu H, Wang G, Qian J. Transcription factors as readers and effectors of DNA methylation. *Nat Rev Genet*. 2016;17.
64. Sinkkonen L, Hugenschmidt T, Berninger P, Gaidatzis D, Mohn F, Artus-Revel CG, et al. MicroRNAs control de novo DNA methylation through regulation of transcriptional repressors in mouse embryonic stem cells. *Nat Struct Mol Biol*. 2008;15(3):259–67.
65. Zhou X, Speer RM, Volk L, Hudson LG, Liu KJ. Arsenic co-carcinogenesis: inhibition of DNA repair and interaction with zinc finger proteins. *Semin Cancer Biol*. 2021;76:86–98.
66. Devesa V, Adair BM, Liu J, Waalkes MP, Diwan BA, Styblo M, et al. Arsenicals in maternal and fetal mouse tissues after gestational exposure to arsenite. *Toxicology*. 2006;224(1–2):147–55.

Publisher's note

Springer Nature remains neutral with regard to jurisdictional claims in published maps and institutional affiliations.